Analytical and Bioanalytical Chemistry (2019) 411:6365–6376
https://doi.org/10.1007/s00216-019-02036-1

RESEARCH PAPER

Enhancing signal and mitigating up-front peptide fragmentation using controlled clustering by gas-phase modifiers

Brendon Seale[1] · Bradley B. Schneider[2] · J. C. Yves Le Blanc[2]

Received: 10 May 2019 / Revised: 9 July 2019 / Accepted: 16 July 2019 / Published online: 17 August 2019

Abstract

Up-front CID fragmentation is a phenomenon where molecular ions are activated and fragment as they enter the atmosphere-to-vacuum region of the mass spectrometer, and consequently can complicate the mass spectra and their analysis. This phenomenon can be minimized by controlling the voltages on lens/optic elements where ions are sampled from the atmospheric region, but this approach can also have a negative effect on overall ion sensitivity. In this study, we introduce gas-phase modifiers (acetonitrile, acetone, cyclohexane, water, and methanol) to the curtain gas to mitigate up-front CID fragmentation. These modifiers cluster with incoming ions, increasing the energy barrier to fragmentation and consequently reducing the complexity of mass spectra. The clustering is monitored by differential mobility spectrometry-mass spectrometry (DMS-MS) and precursor mass spectrum-scanning. Unlike typical singly charged species, peptide ion-modifier clusters were found to survive through the atmosphere-to-vacuum interface of the mass spectrometer, showing that highly charged peptides cluster most strongly with acetonitrile and acetone. In addition, when peptides cluster with acetonitrile, they produce a large increase in signal intensity for the most highly charged and fragile ions. This results in a significant reduction, up to 90% with some modifiers, in up-front CID fragmentation for these fragile highly charged peptides, increasing the overall analytical sensitivity and decreasing the limits of detection by up to 82% depending on the analyte. The proposed technique has no significant detrimental effect on the peptide mass fingerprinting of a BSA or mAb protein digest, but it does reduce the amount of redundant and data-deficient spectra needed to produce adequate sequence coverage using information-dependent acquisition methods by ~40%. We propose that this technique could have a benefit in the fields of proteomics and peptidomics where up-front CID fragmentation and chemical noise routinely mask targets of biological importance.

Keywords Ion clusters · Differential mobility spectrometry · Peptide analysis · Up-front CID fragmentation

Introduction

The analysis of compounds by mass spectrometry (MS) is a ubiquitous technique across many different fields from the detection of pollutants in environmental samples [1–3] to the screening of biological samples for disease conditions [4–6]. Among the many methods for MS ionization is analyte introduction using atmospheric pressure electrospray ionization (ESI). ESI is known to be a low-energy, gentle form of ionization; analytes are ionized but not fragmented in contrast to traditional techniques like electron impact, in which incoming compounds are fragmented from their initial state [7]. But even if ions are formed gently (as in ESI), downstream of ionization, the acceleration of newly formed ions as they move into the vacuum of the mass spectrometer can cause fragmentation of the ions by increasing their internal energy [8, 9]. When this occurs, the phenomenon is frequently referred to as up-front CID fragmentation or up-front CID collision-induced dissociation (up-front CID CID). While this phenomenon can be exploited for many applications (including identification of selected molecule classes for further in-line analysis [10], production of MS/MS data

Published in the topical collection *Close-Up of Current Developments in Ion Mobility Spectrometry* with guest editor Gérard Hopfgartner.

✉ J. C. Yves Le Blanc
Yves.LeBlanc@sciex.com

[1] Department of Chemistry, University of Toronto, 80 St. George St., Toronto, ON M5S 3H6, Canada

[2] SCIEX, 71 Four Valley Drive, Concord, ON L4K 4V8, Canada

on single-stage instruments [11], generation of molecular structural information [12], or toxicology screening [13]), this process is often undesirable, resulting in a decrease in sensitivity for the compound of interest, or in the resulting fragments complicating mass spectra. In especially complex samples like those routinely surveyed for peptidomic or proteomic analyses, it has been suggested that up-front CID fragmentation could account for up to 60% of all non-tryptic peptides [14] in standard protein digest samples and affect more than 15% of metabolites [15] in standard yeast cell lysate metabolomics analyses.

Today, reduction of up-front CID fragmentation is possible by reducing the energetics where the fragmentation occurs [8]. For example, since the majority of fragmentation occurs as ions enter the vacuum region of the instrument, reduction of the inlet potential can limit the fragmentation [16]. The highly energetic environment is caused by accelerating ions through regions with dramatic changes in pressure [17], and this in focusing and declustering incoming ions. A reduction of the inlet potential may also negatively impact the overall signal intensity, resulting in a balance between preventing fragmentation and achieving the highest possible signal. Careful tuning has been shown to improve signal intensity by more than two times [18].

Our approach was inspired by the work of DeMuth et al [19]. who use organic modifiers to shelter non-covalently bound protein complexes. They showed that the introduction of polar organic modifiers to the curtain gas of a nano-ESI source prevented the loss of the heme group of myoglobin and hemoglobin. They proposed that clustering of polar species around the analyte creates a delayed desolvation which prevents fragmentation caused by ion acceleration at the entrance of the mass spectrometer. Addition of stabilization reagents in solution also appears to increase ion stability in the field-free region [20]. We postulate that the same mechanism could be employed on a traditional ESI source to prevent the fragmentation of fragile compounds like highly charged peptides. The clustering of the organic modifier with an analyte necessitates an increase of energy to remove the cluster before fragmentation of the analyte can occur.

In this study, we use gas-phase polar compounds to shelter fragile peptides from fragmentation. We monitor the clustering behavior of five different polar modifiers using differential mobility mass spectrometry (DMS-MS) to (a) prevent fragmentation of a number of peptides and (b) increase the signal intensity of the highest detectable charge state of these peptides. This results in lower limits of detection for these ions and a simplification of the resulting mass spectra, which we propose could greatly aid in peptide searches, as the removal of up-front CID fragmented peptides will leave only those peptides of biological or proteomic relevance behind.

Experimental section

Materials

Peptides human angiotensin I (DRVYIHPFHL, AngI), human angiotensin III (RVYIHPF, AngIII), and bradykinin (RPPGFSPFR), and the proteins bovine serum albumin and trypsin were purchased from Sigma-Aldrich (Oakville, ON, Canada) and used without further purification. Peptide KGAILKGAILR (referred to as "KGAIL") was purchased from SynPep (Dublin, CA, USA) and used without additional purification. Chemical reagents dithiothreitol (DDT), iodoacetamide, ammonium hydroxide, and ammonium bicarbonate were purchased from Sigma-Aldrich (Oakville, ON, Canada). An intact monoclonal antibody (mAb) standard (Waters Intact mAb Mass Check, 720004420EN) was purchased from Waters (Milford, MA, USA). HPLC grade acetonitrile (ACN) and methanol (MeOH) were purchased from Caledon Laboratory Chemicals (Georgetown, ON, Canada). HPLC-grade acetone, cyclohexane, and formic acid (FA) were purchased from Sigma-Aldrich (Oakville, ON, Canada). Distilled, deionized water (resistance ≥ 18 MΩ) was produced in-house by a Millipore Integral 10 water purification system (Billerica, MA, USA).

Protein digestion and LC-DMS-MS instrumentation

A standard trypsin digest of bovine serum albumin (BSA) was performed. Briefly, 100 μL of 20 mM DTT was added to 2 mg of BSA in a polypropylene vial and boiled for 15 min. Then 100 μL of iodoacetamide was added to the vial and it was placed in the dark for 30 min. A 50-mM ammonium bicarbonate/ammonium hydroxide buffer was prepared at pH 8.5 and 600 μL was added to the vial. A total of 39 μg of trypsin was added and the vial was incubated at 37 °C overnight. The resulting digest was diluted to 1 pmol/μL with water containing 0.1% FA for analysis by LC-MS. KGAIL, AngI, AngIII, and bradykinin were added to the diluted BSA digest in some samples to evaluate known fragile peptides (concentrations ranging from 3.4–273, 1.7–133, 4.1–333, and 1.7–133 ng/mL respectively). The digestion procedure was also performed on a monoclonal antibody sample as well, with a final concentration of 1 pmol/μL.

A Shimadzu Prominence LC system equipped with a Phenomenex Aeris 2.6 μm PEPTIDE XB-C18 100 mm × 2.1 mm LC column was coupled to the same LC-MS system used to monitor clustering. Two solvents were employed in a 30-min gradient elution, solvent A: 97.9% water, 2% ACN, 0.1% FA and solvent B: 97.9% ACN, 2% water, 0.1% FA. The gradient elution was as follows: 5% B for 1 min., ramp to 35% B for 14 min, ramp to 60% B for 5 min., ramp to 95% B for 2.5 min., hold B at 95% for

2.5 min., ramp to 5% B in 0.1 min., hold at 5% B for 4.9 min. The column temperature was held at 45 °C and the flow rate was conserved throughout at 0.5 mL/min. Sample injections of 10 μL performed. The ion source conditions were as follows: curtain gas flow of 30 psi, source gases (GS1, GS2) of 50 psi each, source temperature of 450 °C and an ion spray voltage of 5000 V. The MS system was operated in information dependant acquisition (IDA) mode. IDA conditions involved a DMS-ToF-MS survey scan (200 ms) followed by up to 10 DMS-MS/MS scans (30 ms each) on the most intense ions using an intensity threshold of 50 cps. Ions (and isotopes up to 4 Da) were excluded for 2 s. after a single occurrence. The DMS was set to transmission mode (SV = 0) in all IDA experiments.

Data collected from samples containing the spiked peptides were analyzed using PeakView to produce XICs for the 4+, 4+, 3+, and 3+ ions of KGAIL, AngI, AngIII, and bradykinin

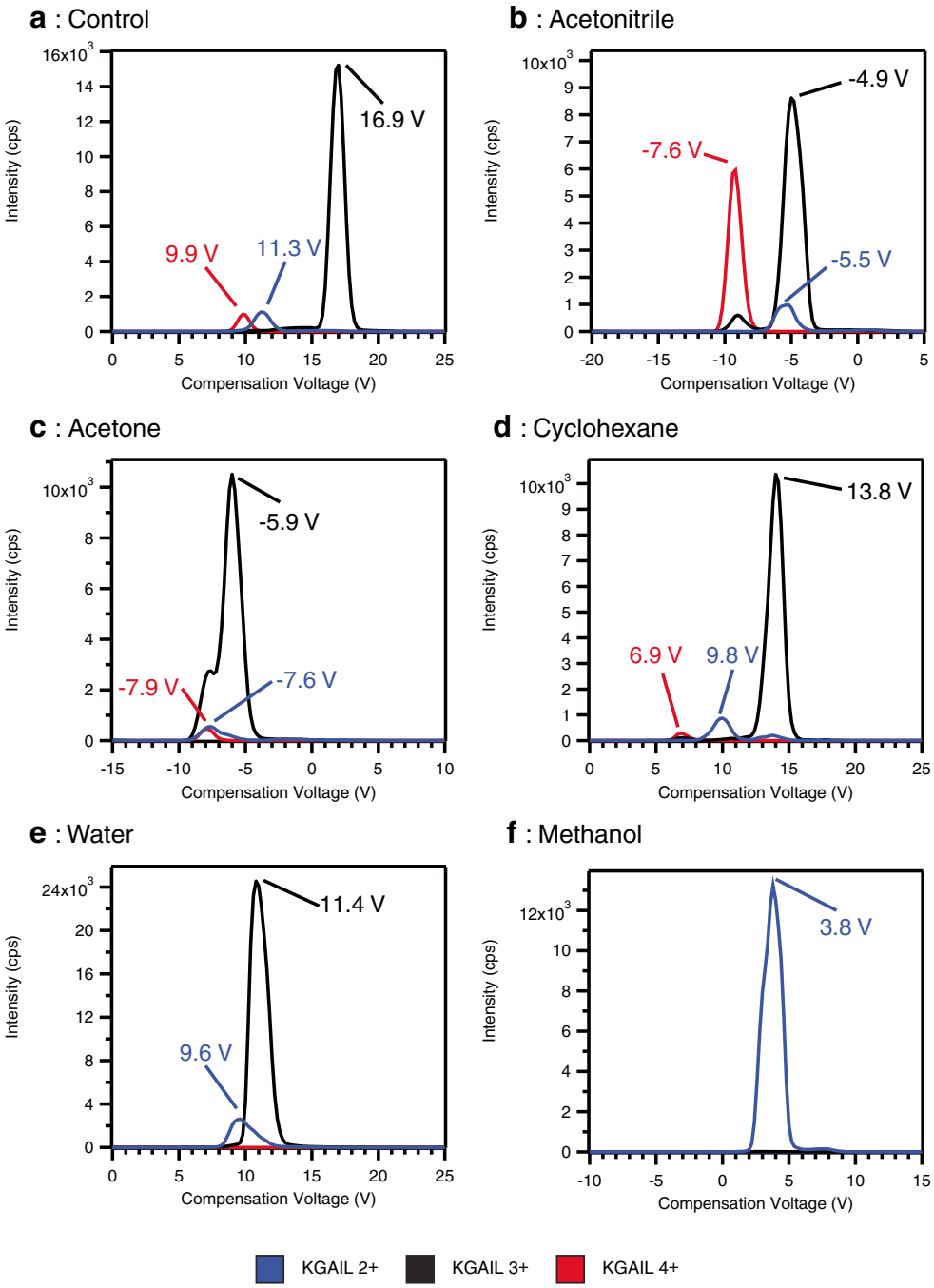

Fig. 1 Ionograms of KGAIL using different curtain gas modifiers. A solution of KGAIL was infused into the instrument and the CV was ramped in 0.2-V increments, with a fixed SV of 3500 V while recoding ToF-MS data. XIC for each of the KGAIL charge states were used to generate the ionograms. **a** The control condition with pure nitrogen shows all ions separated and with positive CVs. **b** In the presence of ACN all CVs shift far negative and the relative intensity of the 4+ ion is increased over the control. **c** The CV range of all ions with acetone is greatly compressed. **d** Cyclohexane exhibits a small CV shift for all ions of ~ 3 V (relative to the control), indicating limited clustering.**e** Water demonstrates a charge stripping effect; the 4+ ion has been lost from the ionogram. **f** Methanol shows an extreme case of charge stripping where only the 2+ ion remains in the ionogram

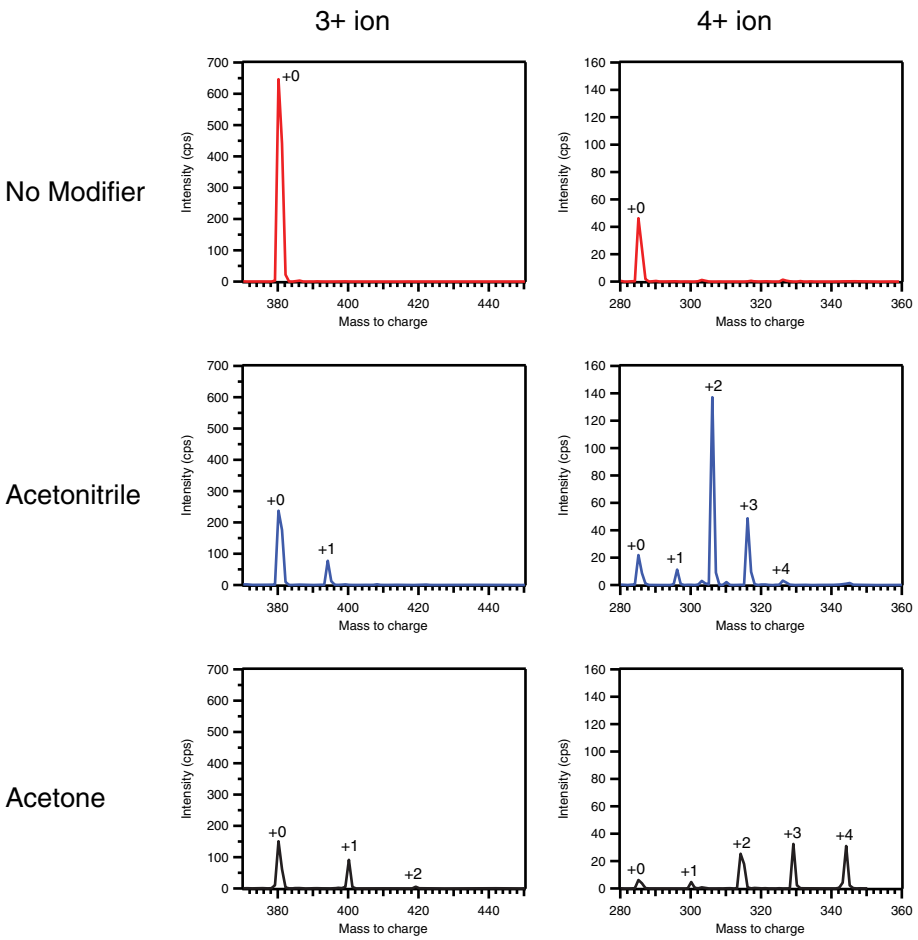

Fig. 2 Precursor spectra of KGAIL 3+ (380.5 *m/z*, left) and 4+ (285.6 *m/z*, right) with nitrogen (red), acetonitrile (blue) and acetone (black). Positive numbers on mass spectra indicate the number of modifier molecules clustered to the selected ion. The spectra indicate that modifier/analyte clusters survive to q1 of the mass spectrometer and are cleared with 10 eV of collision energy in the collision cell before detection (standard operating conditions)

respectively. From the XICs, the peak area of each ion was determined and the mean of three replicates (blank corrected) of four concentrations was subjected to linear regression to produce calibration curves. Limits of detection (LODs) were calculated as the concentration (from the regression) that correlated with the signal of the mean of the blank plus three times the standard deviation of the mean. Data from samples which did not contain additional peptides were analyzed using BioPharmaView v.2.0r3682 (SCIEX) for sequence coverage. Protein sequences were obtained from the UniProt database (P02769) for BSA and from Waters for the mAb sample and sequenced using the Peptide Mapping command (with a maximum charge state of 10+, a minimum peptide length of 3, a deconvolution tolerance of ± 10 ppm, an XIC *m/z* width of 0.075 Da, and automatic recalibration). The percentage of sequence coverage and the percentage of auto-validated sequence coverage (mean of three replicates) were both evaluated by Student's *t* test between samples analyzed in the presence of ACN and controls. The number of IDA counted spectra was determined for each sample using PeakView's IDA Explorer and compared between ACN treatment and control using Student's *t* test.

Modifier clustering

Direct infusion of 1 pmol/μL KGAIL peptide in 50% MeOH and 50% water at a flow rate of 10 μL/min on a SelexION® technology equipped SCIEX 5600+ TripleToF LC-MS system (Concord, ON, Canada) was used to evaluate the different curtain gas modifiers. The ion spray voltage was 5500 V with drying gases (GS1, GS2) flowing at 30 and 15 psi respectively. ToF-MS scans were performed at a declustering potential (DP) of 100 V, collision energy (CE) of 10 eV and an ion transfer coefficient (ITC) of 40% with 250 ms of accumulation time across a *m/z* range of 150–2000 *m/z*. ACN, acetone, MeOH, and cyclohexane

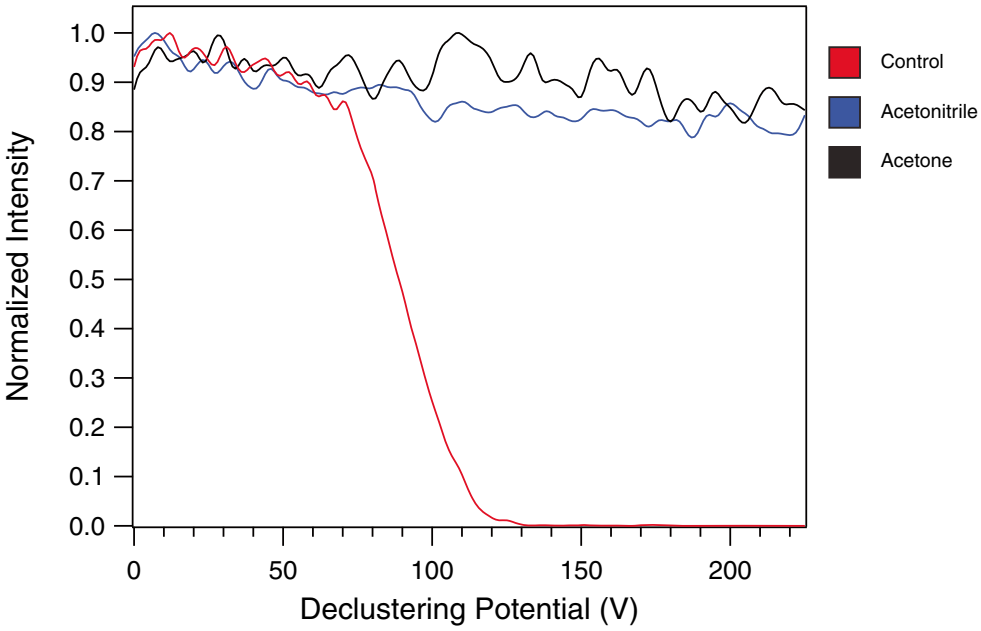

Fig. 3 Infusion DMS-MS DP ramp of XIC of KGAIL 4+ with pure nitrogen transport gas (red), nitrogen with acetonitrile (blue) and, nitrogen with acetone (black). Ramping DP creates artificial up-front CID fragmentation of KGAIL 4+. At standard DP operating conditions (80–100 V) the signal intensity for KGAIL 4+ is reduced by a factor of 2 in the absence of clustering agent. The addition of ACN or acetone eliminates the fragmentation allowing > 85% signal intensity at a 225-V DP. DMS was operated in transmission mode (SV = 0)

were supplied at 1.5% of the 20-psi nitrogen curtain gas using the built-in solvent pump SelexION® DMS controller. The built-in solvent pump delivers the modifier into the curtain gas line, which is then fed into the curtain region prior to the DMS cell. The commercial system provides pump control for the above modifier and ensures delivery at 1.5% and 3.0% in the curtain gas. In the current study, we standardized all analyses at 1.5% level. For water as a modifier, an external Perkin Elmer series 200 micropump (Waltham, MA, USA) was used to supply 37.6 μL/min of water in the curtain gas line operated at 10-psi of nitrogen, resulting in an approximate 1.5% water enriched gas. This was necessary as the built-in pump minimum flow rate would have resulted in a higher percentage of modifier in the gas phase. The DMS internal temperature was kept at 150 °C. All experimental data were collected with the DMS cell mounted and operated either in transparent mode (SV = 0) or at fixed separation voltage (SV) that enabled separation of ions.

Compensation voltage (CV) mapping was performed at a fixed separation voltage (SV) of 3500 V, ramping the CV at 0.2 V increments across an appropriate range. The resulting data were processed by producing extracted ion chromatograms (XIC) of the *m/z* of three separate ions of KGAIL, 4+: 285.6, 3+: 380.5, and 2+: 570.3 with a *m/z* width of 0.3. Gaussian smoothing (1-point width) was applied to each XIC individually. Precursor ion scans were performed of KGAIL under nitrogen without modifier and with ACN and acetone modifiers. Precursor ions for 4+ and 3+ KGAIL (285.6 and 380.5 *m/z*, respectively, width of 2 *m/z*) were acquired with a q1 *m/z* width of 280–360 and 370–450 *m/z* respectively and a scan time of 2 s. A total of 30 scans was acquired and the scans were averaged using Research PeakView v.1.2.2.0 software (SCIEX). DP ramps were performed of KGAIL infusions with ACN, acetone and without any curtain gas modifier using similar MS conditions except the DP was ramped from 0 to 225 V with SV, CV set to 0 V. XICs of 4+ KGAIL were obtained from these scans and plotted. Finally, ToF-MS spectra were obtained of the same infusion of KGAIL under all curtain gas configurations with SV, CV set to 0 V and a fixed DP of 100 V. Spectra were collected for 1 min (119 in total) and the peak area of KGAIL ions and fragments was determined from the average of the collected spectra. Each condition was repeated in triplicate for an assessment of reproducibility and all data was collected using Analyst TF v.1.7.1 (SCIEX).

Results and discussion

Cluster formation and fragmentation reduction

DMS is an effective means of probing clustering behavior of ions [21, 22]. The chemistry of cluster formation amplifies the mobility differences between ions during their high and low field portions of the waveform. Ions which cluster strongly will have very different mobility versus those that cluster weakly. We employed DMS-MS to observe the clustering potential of the KGAIL peptide with ACN, acetone, cyclohexane, water, and MeOH. Figure 1 shows plots of ion intensity as a function of CV for the KGAIL ions (4+ red, 3+ black, and 2+ blue) with different modifiers and a pure nitrogen control at

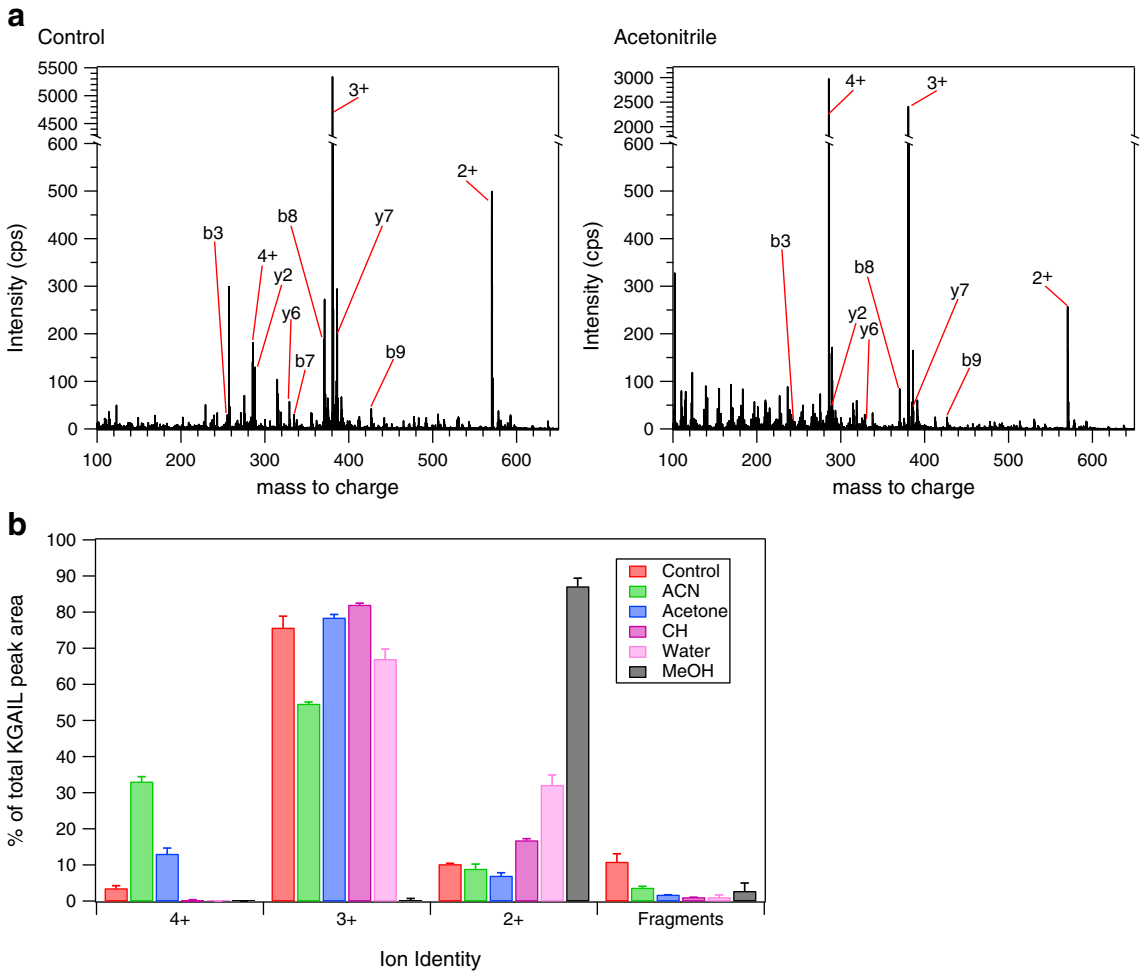

Fig. 4 Fragmentation of KGAIL under different current gas modifiers. **a** Under pure nitrogen control (left) KGAIL shows significant fragmentation of the 4+ ion which results in several b- and y-ions as well as a limited signal for the ion itself. But, with ACN present (right) the intensity of the 4+ ion is dramatically increased while the fragment ions are strongly decreased. **b** The % total peak area from each ion or the sum of all fragments for KGAIL under different modifiers. Both ACN and acetone show an increase in 4+ ion percentage. All organic modifiers limit the total peak area from fragments. MeOH shows most of its peak area from a single state (2+ ion). Error bars represent 1 standard deviation about the mean ($n = 3$). All data were collected in DMS-TOF-MS mode, with DMS operated in transmission mode (SV = 0)

a fixed SV of 3500 V. All the modifiers provided some change in the CV response of KGAIL, with cyclohexane showing the smallest change overall (approximately 3 V less than the control). Polar, aprotic modifiers (ACN, acetone) produced strong negative CV shifts, consistent with other research [23, 24]. It is hypothesized that the strong dipole moment of these modifier compounds (3.92 D and 2.88 D for ACN and acetone, respectively [25]) enables extensive cluster formation on the densely charged KGAIL ions. The signal intensity was also the highest when using ACN. Polar, protic modifiers (MeOH, water) produced weaker negative shifts but also exhibited a proton stripping effect in which the highest charge state ions were suppressed in the resulting ionograms, an effect which has been seen with other protic modifiers [26]. Specifically, using water as a modifier eliminated the 4+ KGAIL ion, while MeOH resulted in the loss of both the 4+ and 3+ ions. Charge stripping can also be seen under other modifiers. For example, at the CV maximum of the 4+ ion with ACN, a small amount of 3+ ion is detected, suggesting a transfer of charge from the 4+ ion to the chemical modifier. Only ACN and acetone showed appreciable amounts of all three charge states (+ 2 to + 4). When data are collected in ToF-MS mode, as those shown in Fig. 1, the ions detected trace their origin from clusters that have undergone declustering in one of two regions where CID can are effectively applied: orifice region and/or collision cell. This approach provides efficient MS information, but may not reflect the ion population that could be selected for MSMS analysis.

Precursor ion scans provide a rudimentary method to observe incoming clustered ions if those clusters survive the entrance to the mass spectrometer. Figure 2 shows representative precursor mass spectra of 4+ and 3+ KGAIL ions for a

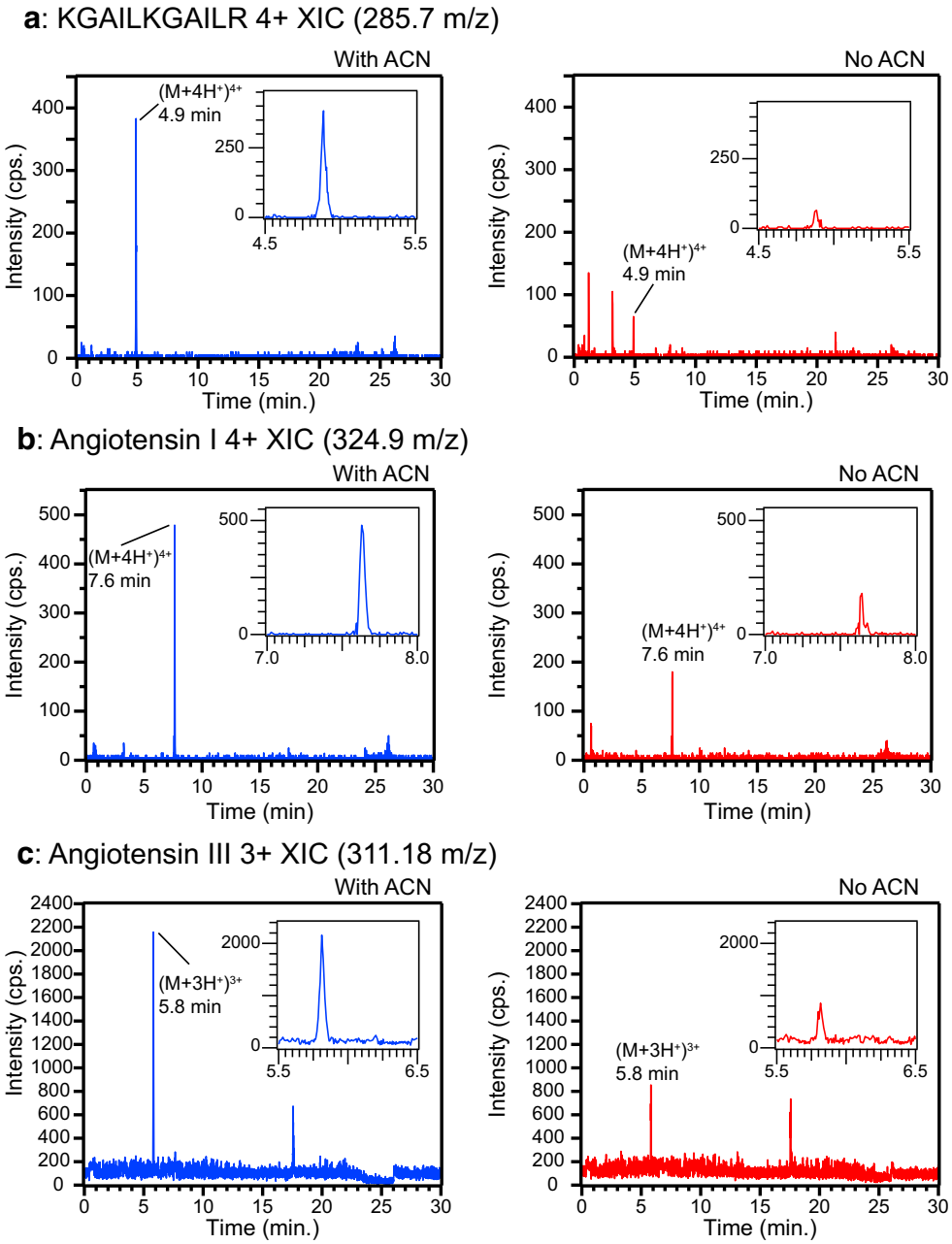

Fig. 5 Selected XIC chromatograms of spiked KGAIL 4+ (285.7 ± 0.3 *m/z*), angiotensin I 4+ (324.9 ± 0.3 *m/z*) and Angiotensin III 3+ (311.18 ± 0.03) ions from BSA digest matrix under ACN (blue) and no modifier (red) conditions. All ions show a marked increase in chromatogram peak area with ACN in the curtain gas. Insets show a zoomed *x*-axis around the ion peaks. **a** KGAIL 4+ has a peak area increase of 5.7× in the presence of the control with a peak area RSD of 8%. **b** Angiotensin I 4+ has a peak area increase of 1.7 times in the presence of ACN with an RSD of the peak area of 6% ($n = 3$). **c** Ang III 3+ has a peak area increase of 2.8 times in the presence of ACN with an RSD of the peak area of 8% ($n = 3$)

nitrogen control, ACN modifier and acetone modifier. The precursor scans were set up to select for the expected *m/z* of the 3+ and 4+ ions (380.5 and 285.6 *m/z* respectively) in q3 while scanning an 80 *m/z* window above those *m/z*s in q1, and the DMS was operated in transmission mode (SV = 0). Control spectra show no clustering (as expected) but with ACN or acetone present, additional peaks beyond the bare ion *m/z* are visible. With ACN, the KGAIL 3+ ion shows a strong peak at the expected ion *m/z* with an additional peak + 14 *m/z* greater than the expected, consistent with the addition of one ACN molecule to the ion. Acetone shows a similar pattern with additional peaks at + 19 and + 38 *m/z* greater than the expected peak, suggesting clusters of one and two additional acetone molecules on the KGAIL ion. Increasing to the 4+ charge state creates a complex set of clusters for ACN and acetone. The 4+ KGAIL precursor scan with ACN shows some bare ion but the predominant signal intensity originates from clusters with 2 or 3 additional ACN molecules, + 21 and + 31.5 *m/z* respectively. Weak signals from clusters with 1 and 4 additional ACN molecules are also present. Acetone shows similarly low amounts of bare ion with stronger signal for clusters of 2, 3, and 4 additional acetone molecules. This evidence shows that ion and modifier clusters can survive into the vacuum of the mass spectrometer, only to be dissociated in the collision cell. This has implications for performing tandem MS experiments on highly charged ions

Table 1 The peak area increases due to the presence of ACN curtain gas modifier on peptide ions spiked into a BSA diges

Ion	Conc. (ng/mL)	Increase w/ACN	%RSD of peak area under ACN
KGAIL 4+	13.6	5.6×	8
AngI 4+	6.7	2.2×	6
AngIII 3+	16.7	2.8×	8
Bradykinin 3+	6.7	1.7×	22

such as KGAIL 4+, as most of the ion intensity is not present (prior to the collision cell) at the expected *m/z* due to significant clustering.

Persistence of cluster is less frequently observed for small molecule (singly charged) and typical modifier such as IPA. The clustering illustrated in Figs. 1 and 2 can be used to reduce the potential for up-front CID fragmentation of ions. To evaluate this phenomenon, up-front CID fragmentation can be induced on our instrument by increasing the DP. Figure 3 shows the effect of increased DP on the XIC of 4+ KGAIL. The control (red, nitrogen only), shows a significant drop in ion intensity beginning at 80 V DP, dropping to less than 40% of the initial intensity at 100 V DP, the default and typical DP used on these instruments. At a DP of 130 V, all the 4+ ion signal is essentially eliminated. Under these conditions, evidence of b and y ion fragments is also seen (see below), which are indicative of up-front CID. In contrast, when ACN or acetone is present, the signal intensity of the 4+ KGAIL is maintained even when high DP values are used. The intensity of the signal at the highest measured potential, 225 V, is still greater than 80% for the peptide with both ACN and acetone. We interpret this result as being evidence that the clustering of the ion shelters it from the energetic process of entering the mass spectrometer. The instability seen under the presence of acetone is likely a function of normal fluctuations in ion signal at relatively low overall intensity as acetone does not exhibit an improvement in 4+ ion intensity.

When full scan mass spectra are collected with DMS set to transmission mode (SV = 0) with nitrogen only, the mass spectrum of 4+ KGAIL ion also shows the presence of b- and y-ions, with b_8, y_4, and y_7 having very strong intensities (Fig. 4a). Upon the addition of ACN to the curtain gas, the intensities of the fragment ions drop and the intensity of the 4+ ion increases (Fig. 4b). The sheltering of the ion (by clustering) seems to have prevented any fragmentation that may occur in the atmosphere-to-vacuum region, resulting in a much stronger signal. Though others have reported on the possibility of using modifier to minimize fragmentation of low molecular weight ions during the transit in the DMS cell [27, 28], the peptide seems to occur after the DMS cell. As the DMS cell SV is increased, there is no systematic decrease in the precursor intensities of either charge state and no indication of increase of fragment ions associated with KGAIL (data not shown). Consequently, it is believed that the fragment ions observed for KGAIL are predominantly generated via up-front CID at the orifice-to-vacuum region. The peak area of all ions and the sum of all peak areas for identifiable fragments were compared to the total peak area derived from KGAIL to evaluate the effect of each modifier (Fig. 4c). Without any modifier, the majority of the KGAIL intensity is from the 3+ charge state but approximately 10% is due to fragment ions. With ACN, the peak area intensity of the KGAIL ions is more evenly distributed, with much stronger 4+ ion than any of the other modifiers. Furthermore, the percentage of the total area derived from fragments is reduced by 66%. Acetone and cyclohexane produce even fewer fragments, with reductions of 84% and 90% respectively. Unfortunately, acetone does not produce as strong a 4+ ion intensity as ACN, and cyclohexane appears to suppress the 4+ ion as well. The charge stripping modifiers water and MeOH produce spectra with enriched 2+ ion intensities at the expense of the other charge states. With MeOH, there is no detectable 4+ or 3+ ion, with 97% of the total peak area from the 2+ ion state. Both the charge stripping modifiers reduce the fragmentation of KGAIL, as observed by the limited amount (2.3 ± 0.7% of the total

Table 2 Limit of detection improvements in fragile ions upon the addition of ACN to the curtain gas

Ion	Limit of detection with no modifier (ng/mL)	Limit of detection with ACN (ng/mL)	Improvement factor
KGAIL 4+*	4.4	3.7	1.19
AngI 4+	5.6	3.6	1.55
AngIII 3+	130	7.7	16.88
Bradykinin 3+	3.9	1.2	3.25

*KGAIL 4+ ion LOD is calculated from a calibration curve covering only three concentrations (3.4 ng/mL, 13.7 ng/mL, and 68.3 ng/mL due to non-linear behavior of the ion

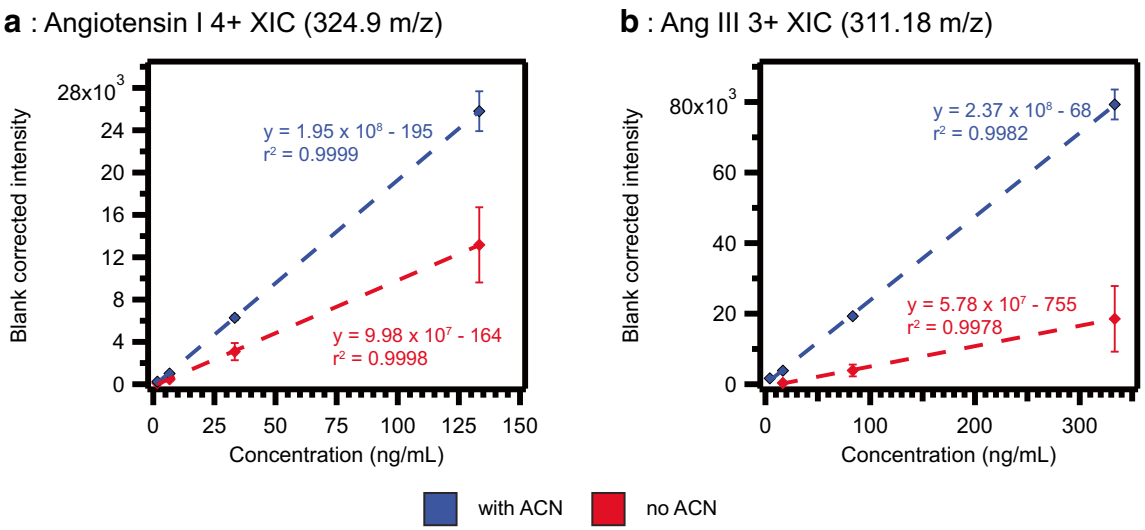

Fig. 6 Calibration curves for Angiotensin I 4+ and Angiotensin III 3+ with ACN modifier and without. The presence of ACN (blue) increases the slope of the calibration line in relation to the control (red). In addition, the uncertainty of the data is greatly reduced with ACN modifier by up to 3 times for AngI 4+ and 6 times for AngIII 3+. **a** Calibration curves for angiotensin I 4+ ion. **b** Calibration curves for Angiotensin III 3+ ion. The lowest point on the curve is omitted from the plot due to its immense uncertainty. Error bars represent 1 standard deviation about the mean (n = 3)

KGAIL area) of fragmentation peak area observed in the ToF-MS spectra (Fig. 4c). Overall, ACN is the most effective modifier in terms of a) reducing up-front fragmentation of the fragile ion and b) enhancing the intensity of the ions with highest charge states (in this case the 4+ charge state).

Application to fragile peptides in protein digests

To assess the application of an ACN curtain gas modifier to a protein digest, four fragile peptides (AngI, AngIII, bradykinin, and KGAIL) were spiked into a BSA digest. This simulates a 'real-world' matrix while still providing a set of analytes with known behavior. It was hypothesized that the presence of the ACN modifier would improve the ability to detect the fragile ions and that the extent of improvement would correlate with the fragility of the ion. Specifically, very fragile ions such as KGAIL 4+ might show very large improvements relative to more stable ions. The samples were analyzed in triplicate by LC-DMS-MS (in transparent mode, SV = 0) with and without the presence of ACN in the curtain gas, and the ions of interest (4+ KGAIL, 3+ bradykinin, 4+ AngI, and 3+ AngIII) were extracted from the chromatograms. Three example-spectra are shown in Fig. 5, KGAIL 4+ (13.7 ng/mL), AngI (6.7 ng/mL), and AngIII (16.7 ng/mL). KGAIL shows a dramatic improvement in peak area under ACN, with a 5.7× increase versus the control, while maintaining an acceptable relative standard deviation (RSD) of the peak < 8% (Fig. 5a). AngI (Fig. 5b) shows a modest improvement in peak area with ACN, approximately 2× over the control condition. When measuring AngIII 3+, the presence of ACN enhances peak area by 2.8× versus the control with only nitrogen (Fig. 5c). In all cases, the CV for replicate injections (n = 3) was < 2%. Table 1 shows the peak area improvement of each spiked ion with an ACN modifier. The scale of each improvement suggests the overall fragility of the ions, with KGAIL 4+ being the most fragile and bradykinin 3+ the least.

The increase in peak area upon the addition of ACN suggests an overall improvement in the sensitivity and detection limit for the fragile ions in question. We propose that this could allow for the detection of previously unknown peptides in biological samples that would otherwise be undetectable due to their fragility. To test this explicitly, calibration curves were collected to determine sensitivities and limits of detection (LODs). All the spiked peptides showed an improvement in their LODs (Table 2) and an increase in the slope of their calibration line. Peptide ions that were previously identified as being very fragile (e.g., KGAIL 4+), show only marginal improvements to their LOD (i.e., a 16% reduction for KGAIL 4+), while the least fragile peptides show dramatic improvements (e.g., AngIII 3+ shows a 94% reduction in LOD). This could be due to an improvement in reproducibility when ACN is present. Figure 6a shows the calibration curves for AngI 4+ ion with ACN (blue) and a control with no modifier (red). The control line has greater uncertainty (with %RSD range across the data points of 26–44% versus a %RSD range across the data points under ACN of 4–15%), likely a combined effect of reduction in matrix interference afforded by the presence of ACN, and reducing fragmentation of the peptide. This is a novel observation which has previously only been reported when the DMS system is engaged for separation [29]. The calibration curve of AngIII is shown in Fig. 6b. The control curve had a

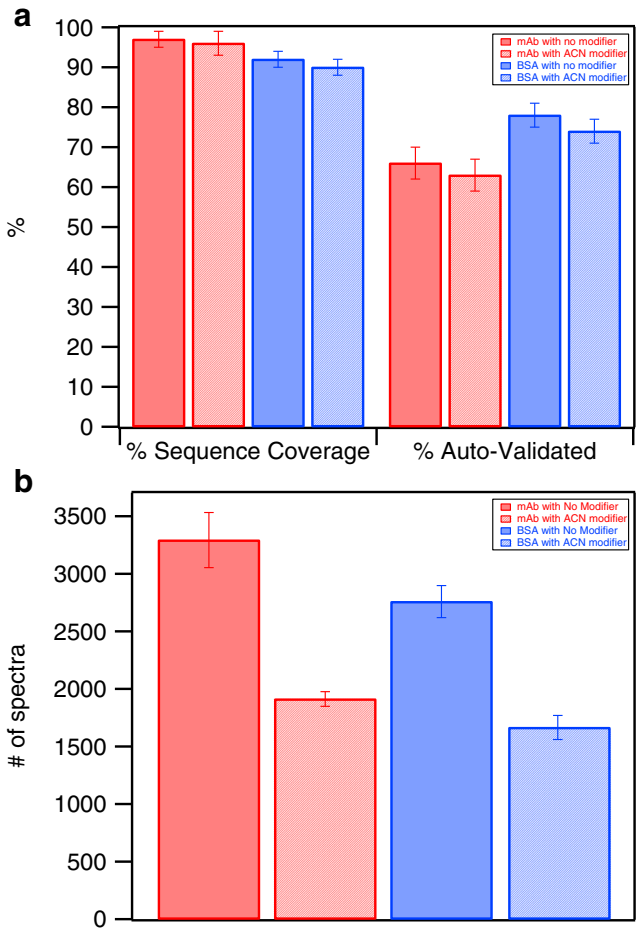

Fig. 7 Protein sequencing comparisons with and without ACN modifier. The sequence coverage of both mAb and BSA were statistically unchanged in the presence of ACN despite the dramatic reduction in the number of spectra captured by IDA. **a** Total MS1 based sequence coverage and % of computer auto-validated sequence coverage was no different with ACN. **b** The total number of spectra captured by the IDA method. The presence of ACN reduces the total number of IDA "hits" necessary to achieve maximal coverage. Error bars represent 1 standard deviation about the mean ($n = 3$)

substantially larger LOD (130 ng/mL vs. 7.7 ng/mL with ACN present). The benefit is likely due to a reduction to the relative standard deviation (RSD) at each measured point. The control data had approximately ~ 50% RSD at each data point vs. 1–8% RSD when measured with ACN present. In combination with an increase in peak area, this results in much improved detection limit using ACN for this charge state.

The benefits of using ACN to increase sensitivity do not negatively impact the results of peptide mass fingerprinting of the protein matrix. Figure 7a shows the % sequence coverage determined by BioPharmaView's algorithm, which matches *m/z* of potential peptides in MS1, for a digest of a mixture of a mAb (chosen as a stand-in for common protein therapeutics) and BSA (chosen to represent a generic protein), analyzed with and without an ACN modifier. Statistically, there is no difference between the sequence coverage with the modifier for the mAb ($p = 0.363$, $\alpha = 0.05$) or BSA ($p = 0.224$, $\alpha = 0.05$). A similar result is seen with BioPharmaView's auto-validation algorithm which employs MS/MS spectra to verify its matches in MS1. Specifically, there is no significant impact on the auto-validated sequence coverage for the mAb ($p = 0.410$, $\alpha = 0.05$) or BSA ($p = 0.172$, $\alpha = 0.05$) when using ACN as a modifier. This suggests that the clustering seen in Fig. 2 does not have a detrimental impact on most of the peptides present in the sample. However, it remains possible that there are some peptides that cannot be detected in MS/MS scans using IDA due to their *m/z* being altered by clustering. This is because the IDA method selects for the exact *m/z* of the precursor, which would only be detected after declustering in the collision cell. Stated another way, in this case, Q1 would be effectively set at different, erroneous mass. Thus, data-independent acquisition (DIA) methods such as Sequential Window Acquisition of All THeoretical mass spectra (SWATH) [30] with sufficiently wide isolation windows may be necessary to achieve complete MS/MS information from samples analyzed with strongly clustering modifiers like ACN or acetone.

Another major benefit of using ACN as a modifier for the IDA method is a significant reduction in the number of spectra captured in the analysis (Fig. 7b). Both the mAb and BSA digests had large reductions in the total number of IDA events using ACN when compared to the control (reductions of 42% and 40% respectively). This indicates that a good portion of the spectra collected by IDA do not add further support for the identification of the protein. We speculate that these extraneous spectra (that are not identified when using ACN) may be derived from contaminants and noise which is eliminated by the gas-phase modifier (Figs. 5 and 6) or peptide fragments created by up-front CID fragmentation (Fig. 4). The eliminated spectra provide either no support for protein identification or redundant support. The removal of these artifact spectra could be of great benefit to more complex analyses where elimination of noise is crucial to proper interpretation of the biological significance of proteins and peptides.

Conclusion

We have demonstrated the use of polar gas-phase modifiers in the curtain gas to shelter fragile peptide ions from up-front CID fragmentation. The modifiers cluster with the ions which results in a larger energy barrier to fragmentation which we can monitor via DMS and precursor scans. The net result is significant reduction in fragmentation of fragile ions which leads to a decrease in limits of detection for these ions in a protein digest matrix. Furthermore, this method does not interfere with routine peptide mass

fingerprinting of the protein digest and causes a reduction in the number of redundant spectra produced by IDA means of MS/MS acquisition. Since the reduction in the number of MSMS collected did not lead to a reduction in the total number of spectra that lead to confirmation of the detected protein, we anticipate this approach to be beneficial in tryptic digest analysis. The impact of the proposed workflow on biological analysis of more complex samples will be part of a future study.

Acknowledgments We thank Dr. Larry Campbell (SCIEX, Concord, ON) for fruitful discussions. BS thanks the Natural Sciences and Engineering Research Council of Canada (NSERC), specifically the CREATE MS-ESE training program and Professor Derek Wilson (York University, Toronto, ON) for funding. BS also thanks the province of Ontario for an Ontario Graduate Scholarship (OGS). BS thanks Aaron Wheeler (University of Toronto, Toronto, ON) for discussion and support as his PhD supervisor.

Compliance with ethical standards

No biological material was used in the present work.

Conflict of interest The authors declare that they have no conflict of interest.

References

1. Shen F, Wang L-H, Zhou Q, Huang X-H, Zhang J-Z, Zhu P-Y, et al. Simultaneous determination of aniline, benzidine, microcystins, and carbaryl in water using ultra-performance liquid chromatography–electrospray ionization tandem mass spectrometry. Water Air Soil Pollut. 2017;228:69. https://doi.org/10.1007/s11270-017-3260-5.
2. Wood TP, Du Preez C, Steenkamp A, Duvenage C, Rohwer ER. Database-driven screening of south African surface water and the targeted detection of pharmaceuticals using liquid chromatography - high resolution mass spectrometry. Environ Pollut. 2017;230:453–62. https://doi.org/10.1016/j.envpol.2017.06.043.
3. Campos-Mañas MC, Plaza-Bolaños P, Sánchez-Pérez JA, Malato S, Agüera A. Fast determination of pesticides and other contaminants of emerging concern in treated wastewater using direct injection coupled to highly sensitive ultra-high performance liquid chromatography-tandem mass spectrometry. J Chromatogr A. 2017;1507:84–94. https://doi.org/10.1016/j.chroma.2017.05.053.
4. Liao H-C, Chan M-J, Yang C-F, Chiang C-C, Niu D-M, Huang C-K, Gelb MH, Mass spectrometry but not fluorimetry distinguishes affected and pseudodeficiency patients in newborn screening for Pompe disease. Clin. Chem. 63 (2017). doi: https://doi.org/10.1373/clinchem.2016.269027.
5. Clark ZD, Cutler JM, Pavlov IY, Strathmann FG, Frank EL. Simple dilute-and-shoot method for urinary vanillylmandelic acid and homovanillic acid by liquid chromatography tandem mass spectrometry. Clin Chim Acta. 2017;468:201–8. https://doi.org/10.1016/j.cca.2017.03.004.
6. Saville JT, Smith NJC, Fletcher JM, Fuller M. Quantification of plasma sulfatides by mass spectrometry: utility for metachromatic leukodystrophy. Anal Chim Acta. 2017;955:79–85. https://doi.org/10.1016/j.aca.2016.12.002.
7. Banerjee S, Mazumdar S. Electrospray ionization mass spectrometry: a technique to access the information beyond the molecular weight of the analyte. International Journal of Analytical Chemistry 2012;2012:1–40. https://doi.org/10.1155/2012/282574.
8. Gabelica V, De Pauw E. Internal energy and fragmentation of ions produced in electrospray sources. Mass Spectrom Rev. 2005;24:566–87. https://doi.org/10.1002/mas.20027.
9. Vékey K. Internal energy effects in mass spectrometry. J Mass Spectrom. 1996;31:445–63. https://doi.org/10.1002/(SICI)1096-9888(199605)31:5<445::AID-JMS354>3.0.CO;2-G.
10. Liu Y, Pereira ADS, Martin JW. Discovery of C5-C17 poly- and perfluoroalkyl substances in water by in-line Spe-HPLC-Orbitrap with up-front CID fragmentation flagging. Anal Chem. 2015;87:4260–8. https://doi.org/10.1021/acs.analchem.5b00039.
11. Abrankó L, García-Reyes JF, Molina-Díaz A. Up-front CID fragmentation and accurate mass analysis of multiclass flavonoid conjugates by electrospray ionization time-of-flight mass spectrometry. J Mass Spectrom. 2011;46:478–88. https://doi.org/10.1002/jms.1914.
12. Nuengchamnong N, Sookying S, Ingkaninan K. LC-ESI-QTOF-MS based screening and identification of isomeric jujubogenin and pseudojujubogenin aglycones in Bacopa monnieri extract. J Pharm Biomed Anal. 2016;129:121–34. https://doi.org/10.1016/j.jpba.2016.06.052.
13. Marquet P, Venisse N, Lacassie É, Lachâtre G. Up-front CID CID mass spectral libraries for the "general unknown" screening of drugs and toxicants. Analysis. 2000;28:925–34. https://doi.org/10.1051/analusis:2000280925.
14. Fang P, Liu M, Xue Y, Yao J, Zhang Y, Shen H, et al. Controlling nonspecific trypsin cleavages in LC-MS/MS-based shotgun proteomics using optimized experimental conditions. Analyst. 2015;140:7613–21. https://doi.org/10.1039/C5AN01505G.
15. Xu Y-F, Lu W, Rabinowitz JD. Avoiding misannotation of up-front CID fragmentation products as cellular metabolites in liquid chromatography–mass spectrometry-based metabolomics. Anal Chem. 2015;87:2273–81. https://doi.org/10.1021/ac504118y.
16. Loo JA, Udseth HR, Smith RD, Futrell JH. Collisional effects on the charge distribution of ions from large molecules, formed by electrospray-ionization mass spectrometry. Rapid Commun Mass Spectrom. 1988;2:207–10. https://doi.org/10.1002/rcm.1290021006.
17. Weinmann W, Stoertzel M, Vogt S, Wendt J. Tune compounds for electrospray ionisation/up-front CID collision-induced dissociation with mass spectral library searching. J Chromatogr A. 2001;926:199–209. https://doi.org/10.1016/S0021-9673(01)01066-4.
18. Puchalska P, Luisa Marina M, Concepción García M. Development of a high-performance liquid chromatography–electrospray ionization-quadrupole-time-of-flight-mass spectrometry methodology for the determination of three highly antihypertensive peptides in maize crops. J Chromatogr A. 2013;1285:69–77. https://doi.org/10.1016/j.chroma.2013.02.015.
19. DeMuth JC, Bu J, McLuckey SA. Electrospray droplet exposure to polar vapors: delayed desolvation of protein complexes. Rapid Commun Mass Spectrom. 2015;29:973–81. https://doi.org/10.1002/rcm.7188.
20. Lemaire D, Marie G, Serani L, Laprévote O. Stabilization of gas-phase noncovalent macromolecular complexes in electrospray mass spectrometry using aqueous triethylammonium bicarbonate buffer. Anal Chem. 2001;73:1699–706. https://doi.org/10.1021/AC001276S.

21. Schneider BB, Covey TR, Coy SL, Krylov EV, Nazarov EG. Chemical effects in the separation process of a differential mobility/mass spectrometer system. Anal Chem. 2010;82:1867–80. https://doi.org/10.1021/ac902571u.
22. Eiceman G, Krylov E, Krylova NS, Nazarov EG, Miller RA. Separation of ions from explosives in differential mobility spectrometry by vapor-modified drift gas. Anal Chem. 2004;76:4937–44. https://doi.org/10.1021/AC035502K.
23. Schneider BB, Nazarov EG, Covey TR. Peak capacity in differential mobility spectrometry: effects of transport gas and gas modifiers. Int J Ion Mobil Spectrom. 2012;15:141–50. https://doi.org/10.1007/s12127-012-0098-9.
24. Blagojevic V, Chramow A, Schneider BB, Covey TR, Bohme DK. Differential mobility spectrometry of isomeric protonated dipeptides: modifier and field effects on ion mobility and stability. Anal Chem. 2011;83:3470–6. https://doi.org/10.1021/ac200100s.
25. W.M. Haynes, ed., Molecular structure and spectroscopy, in: CRC Handb. Chem. Phys., 97th ed., CRC Press/Taylor & Francis, Boca Raton, 2017.
26. Zhu S, Campbell JL, Chernushevich I, Le Blanc JCY, Wilson DJ. Differential mobility spectrometry-hydrogen deuterium exchange (DMS-HDX) as a probe of protein conformation in solution. J Am Soc Mass Spectrom. 2016;27:991–9. https://doi.org/10.1007/s13361-016-1364-6.
27. Kendler S, Lambertus GR, Dunietz BD, Coy SL, Nazarov EG, Miller RA, et al. Fragmentation pathways and mechanisms of aromatic compounds in atmospheric pressure studied by GC–DMS and DMS–MS. Int J Mass Spectrom. 2007;263:137–47. https://doi.org/10.1016/j.ijms.2007.01.011.
28. Beach DG. Differential mobility spectrometry for improved selectivity in hydrophilic interaction liquid chromatography-tandem mass spectrometry analysis of paralytic shellfish toxins. J Am Soc Mass Spectrom. 2017;28:1538–0. https://doi.org/10.1007/s13361-017-1651-x.
29. Schneider BB, Covey TR, Nazarov EG. DMS-MS separations with different transport gas modifiers. Int J Ion Mobil Spectrom. 2013;16:207–16. https://doi.org/10.1007/s12127-013-0130-8.
30. Gillet LC, Navarro P, Tate S, Röst H, Selevsek N, Reiter L, et al. Targeted data extraction of the MS/MS spectra generated by data-independent acquisition: a new concept for consistent and accurate proteome analysis. Mol Cell Proteomics. 2012;11:O111.016717. https://doi.org/10.1074/mcp.O111.016717.